Full-Wave Spectral-Domain Computation of Material, Radiation, and Guided Wave Losses in Infinite Multilayered Printed Transmission Lines

Nirod K. Das and David M. Pozar, *Fellow, IEEE*

Abstract—**A unified solution for full-wave computation of losses in a general multilayered planar transmission line is presented. It includes material losses (dielectric and conductor losses), losses due to radiation leakage, and losses caused by leakage of power to source-free characteristic modes (surface wave or waveguide modes, for example) of the multilayered geometry. A spectral-domain moment method is used with the Galerkin testing procedure. Significant modification of the conventional spectral-domain analysis of planar transmission lines is necessary in enforcing proper boundary conditions in the Galerkin testing procedure and, what is more important, in accounting for poles and branch cuts in the complex Fourier transform domain in order to rigorously account for the different loss mechanisms discussed above. Results for a few representative geometries, namely strip and/or material loss in a microstrip line and a slotline, surface parallel plate mode leakage loss in a conductor-backed slotline and a two-layer stripline, and radiation loss in a single and a coupled stripline at the interface between two infinite mediums, are presented to demonstrate these various loss effects.**

I. Introduction

PRINTED transmission lines in multiple layers of dielectrics and/or ground planes are of interest for multilayered architectures of integrated phased arrays [1]–[3]. Considering the potential millimeter-wave applications, not only the material losses (dielectric and conductor losses) in the transmission line (which result in significant loss in the feed network of a phased array), but also losses caused by possible leakage of power to radiation or to the modal fields of the layered structure (sometimes unexpected, though inevitable), need to be studied. Characterization of such material, modal, and radiation losses is also of importance for integrated optoelectronic applications in studying propagation of picosecond pulses along a printed transmission line caused by the large frequency contents of the short pulses [4], [5]. A full-wave characterization of these integrated loss effects for an arbitrary multilayered printed transmission line is warranted.

Spectral-domain analyses have been successfully demonstrated and widely used for planar transmission lines [6]–[10]. These solutions usually solve for a real propagation constant, assuming various conductors and dielectric media to be ideally lossless. The losses due to the nonideal dielectrics and conductors can be separately calculated using a conventional perturbation analysis [10], [11] or other semiempirical formulas [12], [13] (applicable for single-layered microstrip line only). However, such perturbation analyses assume a small loss, which may be generally true in many practical applications, but one does not know *a priori* the range of validity of the small-loss assumption. Also, for plananr transmission lines with multiple layers of dielectrics and ground planes, where the use of a perturbation analysis requires adding loss contributions from each individual dielectric or conducting layer, the calculation becomes increasingly complex from a computational point of view as the number of layers increases.

Full-wave computation of dielectric and conductor loss can, however, be implemented in the spectral domain [9], [14] by replacing the dielectric constants with their respective complex values, accounting for finite conductivity of infinite ground planes by enforcing the proper impedance boundary condition, and solving for the complex propagation constant —in contrast to a real propagation constant in the lossless case. This seemingly involves the numerical complexity of root searching in the two-dimensional complex propagation constant plane, and also (as reported to date) cannot generally include the loss caused by finite conducting strips of finite thickness (of the order of skin depth) in a full-wave sense (for example, due to the conducting strip of a microstrip line and the conducting edge of a slotline). In practice, however, for most cases the loss caused by the sharp edges of finite conducting strips contributes significantly to the total loss. In some integrated circuit applications, the strip thickness is actually of the order of a skin depth. Hence, in these cases, the previously reported spectral-domain loss analyses are not very useful.

In addition to the conventional material losses caused by dissipation of power in imperfect dielectrics and conductors, losses to dominant modes of infinite-length planar transmission lines can result from leakage of power to radiation or characteristic surface modes. These nonconventional losses, usually undesirable, are sometimes inevitable for high-frequency applications and for certain multilayered configurations of planar transmission lines. For example, leakage of power in a conductor-backed slotline to the parallel-plate waveguide mode has recently been reported in [15], and has been characterized using a mode matching technique. This

Manuscript received March 30, 1990; revised August 7, 1990.

N. K. Das was with the Department of Electrical and Computer Engineering, University of Massachusetts at Amherst, Amherst, MA. He is now with Polytechnic University, Route 110, Farmingdale, NY 11735.

D. M. Pozar is with the Department of Electrical and Computer Engineering, University of Massachusetts at Amherst, Amherst, MA 01003.

IEEE Log Number 9040561.

0018-9480/91/0100-0054$01.00 ©1991 IEEE

leakage effect unconditionally occurs for the dominant mode of the conductor-backed slotline at all frequencies but can be minimized by increasing the thickness of the parallel-plate structure. The dominant mode of an infinite-length stripline structure with two different dielectric substrates on the two sides of its center conductor can experience an equivalent leakage to the parallel-plate TEM mode [2]. It has been found that this can occur if the substrate with the larger dielectric constant is thicker than the other substrate [16]. Similar loss for the dominant transmission line mode can conditionally occur for higher frequencies, for example in a coplanar stripline on a finite-thickness dielectric substrate, owing to leakage to surface waves on the substrate [4], [5]. Loss in a coplanar stripline at the interface of two semi-infinite mediums caused by radiation of power to the medium with higher dielectric constant is described in [17] and analyzed using a simplified reciprocity method. Leakage loss can also occur for higher order modes in a single-layered microstrip [18]–[20], but seems to be very weakly excited for practical substrate thicknesses by conventional probe launching in comparison with the dominant microstrip mode. This problem of leaky higher order modes in a single-layered microstrip line is of direct theoretical relevance to the present work, but owing to their high impedance characteristics the modes are of less immediate practical relevance in integrated circuit applications.

For a general architecture of a multilayered integrated phased array [1]–[3], [16] the characteristic source-free surface modes can exist in a variety of forms, such as a surface wave mode, a parallel-plate waveguide mode, or other forms of trapped surface modes of the multilayered geometry [16]. Loss in a multilayered transmission feed network arising from possible leakage to any of these modes should be carefully predicted and probably quantified to help suppress or avoid a potential disaster in the practical design.

This paper presents a unified spectral-domain moment analysis of various possible loss mechanisms in a general multilayered printed transmission line. The analysis is full wave in all respects and establishes a general analytical framework to account for one or more of the possible loss mechanisms discussed earlier in the spectral domain. The various steps of a conventional spectral-domain analysis need to be revisited and suitably modified to rigorously account for these effects. It is seen that the fields of an infinite transmission line with surface leakage or radiation leakage exponentially grow in the transverse or the normal direction, respectively. (This phenomenon, however, never occurs for real finite-length transmission lines, and should not be misunderstood to violate the radiation condition for finite structures.) Section II describes the analysis, with specific results presented in Section III for a) strip and material loss in a microstrip and a slotline, b) parallel-plate leakage loss in a conductor-backed slotline and a two-layer stripline, and c) radiation leakage loss in a single microstrip line or an odd-mode coplanar stripline at the interface of a semi-infinite dielectric. Various critical points are discussed from analytical and qualitative viewpoints.

II. Analysis

In performing a spectral-domain moment method solution for a printed transmission line geometry, one needs to expand the unknown electric currents or equivalent magnetic currents (electric field) of the system with an N-dimensional basis set and enforce suitable boundary conditions via a variational Galerkin testing procedure [7], [8]. The testing procedure establishes a set of linear equations:

$$\sum_{i=1}^{N} I_i Z_{ij}(k_e) = 0, \qquad j = 1, N. \tag{1}$$

As a result, it is required to solve for the root, k_e, of a determinant:

$$\mathrm{Det}\left[Z_{ij}(k_e)\right]_{N\times N} = 0 \tag{2}$$

where Z_{ij} is the reaction of suitable field component(s) due to the ith expansion function on the jth testing function. The testing functions are chosen to be the same as the expansion functions for a Galerkin testing method. In the spectral domain the Z_{ij}'s are obtained by evaluating Fourier integrals that involve transforms of the basis functions chosen and the spectral-domain Green's functions to account for the field components for proper boundary condition testing. Thus, the entire procedure involves four basic steps: 1) obtaining the Green's function, 2) formulating the testing procedure, 3) evaluating the necessary spectral integrations, and 4) performing the root searching. These four steps used in a conventional moment method analysis need to be critically viewed to account for all possible loss mechanisms. As will be discussed, choosing the proper Green's functions in step 1 can account for any losses due to infinite (in lateral extent) conductors or substrates; using a suitable testing procedure in step 2 can account for losses caused by finite-width and finite-thickness conducting strips or by slot edges; and properly deforming the contour of spectral integration of step 3 in the complex spectral plane can rigorously account for possible radiation or characteristic mode leakage effects. Deformation of the integration contour to circumvent the characteristic wave poles incorporates the leakage loss due to excitation of these modes, whereas deformation of the integration contour with proper selection of the branch plane and branch cut can incorporate any radiation loss. Finally, the complex root searching procedure, which is generally computationally intensive, can be greatly simplified for small losses through the use of a simple method called the spectral-domain perturbation technique. This technique uses the simplicity of real root finding (as in a lossless case) but has the added power of incorporating all integrated loss effects without additional computation.

A. The Green's Function

As discussed, the Green's functions are necessary to account for different field components in the testing procedure to evaluate the spectral integrals for Z_{ij}. Through these Green's functions, the effect of the layered medium is rigorously incorporated into the solution. Thus, any material loss in the dielectric substrates or infinite (in lateral extent) lossy ground planes can be accounted for by using Green's functions with complex dielectric constants and finite ground plane conductivity. Such Green's functions can be easily derived using the iterative method presented in [21], with details for its most general dyadic form with all possible source and field components in [16]. Unlike the Green's functions with perfect conducting planes that satisfy zero tangential field boundary conditions on the perfectly conducting ground planes, impedance tangential boundary conditions are enforced for imperfect conductors of infinite thickness (or significantly thicker than the skin depth). Finite

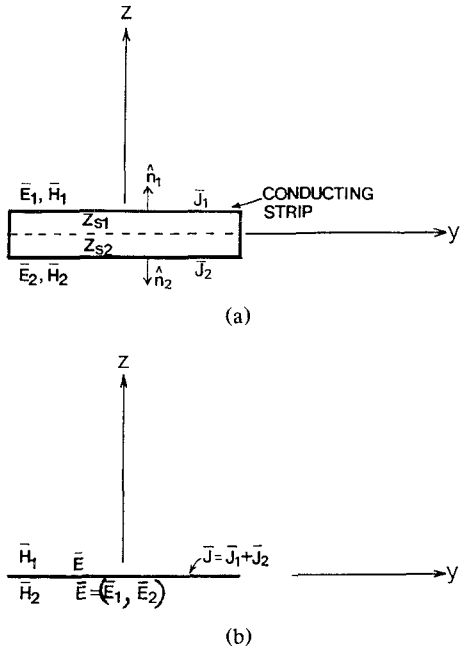

Fig. 1. Thin-strip equivalent problem for a conducting strip showing the equivalence between the tangential electric field boundary conditions. (a) Original problem. (b) Thin-strip equivalent problem.

field leakage through finite-thickness conductors can be accounted for by treating the conductor as another dielectric layer with a complex dielectric constant. Complex magnetic permeabilities are as easily incorporated to account for any magnetic losses, if desired. Certain types of anisotropic losses (uniaxial) in dielectric substrates can also be incorporated into the Green's functions of [16] via complex dielectric or magnetic tensors, as long as the TE and TM waves are not coupled to each other in the substrate layers.

B. Boundary Conditions for Galerkin Testing

The boundary conditions used for conventional solutions use vanishing electric fields on the strip conductors for microstrip-type geometries. For slot geometries, where an aperture electric field formulation is used, continuity of the tangential magnetic field across the slot (or, equivalently, zero electric current on the slot region) is the boundary condition usually required [9]. The magnetic fields are computed without accounting for the finite conductivity of the conductors present in the plane of the slot.

Such boundary conditions for strip-type or slot-type transmission lines, as expected, cannot account for the significant conductor loss in the vicinity of the finite strip guiding structure. A modified set of boundary conditions is given below which can, however, potentially account for these losses via Galerkin testing. A similar method has been very recently reported in [22] for strip conductors only.

Let the surface currents on the top and bottom surfaces of a lossy conducting strip be, respectively, $\bar{J}_1(y)e^{-jk_c x}$ and $\bar{J}_2(y)e^{-jk_c x}$. Assuming the strip to be thin, the surface currents on the top and bottom can be equivalently replaced by a single strip of surface current $\bar{J}(y)e^{-jk_c x} = (\bar{J}_1(y) + \bar{J}_2(y))e^{-jk_c x}$ (see Fig. 1). In order for $\bar{J}_1$ and $\bar{J}_2$ or, equivalently, $\bar{J}$ be the eigencurrents of the system, the total tangential electric field on the two surfaces of the conductor should be related to the corresponding magnetic fields by the impedance boundary conditions:

$$\bar{E}_1 = Z_{s1}(\hat{n}_1 \times \bar{H}_1) \qquad \bar{E}_2 = Z_{s2}(\hat{n}_2 \times \bar{H}_2) \tag{3}$$

where Z_{s1} and Z_{s2} are the complex surface impedances of the top and bottom surfaces (this would account for different surface metallizations on the two sides). Now, with the equivalent eigencurrents, $\bar{J} = \bar{J}_1 + \bar{J}_2$, at the center of the strip, the above impedance boundary conditions can be equivalently enforced at the center of the strip as

$$\bar{E} \simeq (\bar{E}_1, \bar{E}_2) \tag{4a}$$

where the right-hand side is the weighted average of the tangential electric fields, $\bar{E}_1$ and $\bar{E}_2$. Such a weighted averaging can be equivalently implemented in spectral domain as

$$\tilde{\bar{E}} \simeq (\tilde{\bar{E}}_1, \tilde{\bar{E}}_2) = \hat{x}\frac{|\tilde{E}_{1x}|\tilde{E}_{1x} + |\tilde{E}_{2x}|\tilde{E}_{2x}}{|\tilde{E}_{1x}| + |\tilde{E}_{2x}|} + \hat{y}\frac{|\tilde{E}_{1y}|\tilde{E}_{1y} + |\tilde{E}_{2y}|\tilde{E}_{2y}}{|\tilde{E}_{1y}| + |\tilde{E}_{2y}|}. \tag{4b}$$

Using (3) this equivalent impedance boundary condition can be variationally implemented by a Galerkin's test procedure (eq. (1)):

$$\sum_{i=1}^{N} I_i \int \left[\tilde{\bar{E}}_i - \hat{z} \times \left(Z_{s1}\tilde{\bar{H}}_1, -Z_{s2}\tilde{\bar{H}}_2\right)\right] \cdot \tilde{\bar{J}}_j^* \, dk_y = \sum_{i=1}^{N} I_i Z_{ij} = 0 \tag{5}$$

where the tilde ($\sim$) represent the Fourier transform quantities with respect to y, $\tilde{J}_j$ is the transform of the jth basis function, and the subscript i corresponds to fields due to the ith basis function, with unknown amplitude I_i.

For the above derivations it is assumed that the strip thickness is larger than several skin depths; thus the surface electric fields are dependent only on the magnetic field at that surface by the surface impedance. This would not be true if the strip thickness were of the order of a skin depth, where the tangential electric and magnetic fields on the two surfaces are coupled to each other via an impedance matrix. Using plane wave transmission characteristics through a thin conducting layer (in terms of an impedance matrix $[Z]$),

$$Z_{11} = Z_{22} = -jZ_s \cot \beta_m t \qquad Z_{12} = Z_{21} = jZ_s \operatorname{cosec} \beta_m t \tag{6}$$

$$\bar{E}_1 = \hat{z} \times (Z_{11}\bar{H}_1 + Z_{12}\bar{H}_2) \qquad \bar{E}_2 = -\hat{z} \times (Z_{21}\bar{H}_1 + Z_{22}\bar{H}_2) \tag{7}$$

where β_m is the complex propagation constant, Z_s is the complex surface impedance, and t is the thickness of the metal strip. Equation (7) gives the new set of impedance boundary conditions on the two surfaces of the conductor, for which a weighted average similar to (4) can be obtained to give the equivalent electric field boundary condition for the thin-strip approximation.

The equivalent problem for the electric field in a slot on a lossy ground plane is shown in Fig. 2. With the assumption that the tangential magnetic fields in the slot region of the original problem are zero, the equivalent problem for the slot region can be represented only with magnetic currents, $\bar{M} = \bar{E} \times \hat{z}$. Using the general principle of equivalent surface current modeling, we can place the lossy conducting plane between the equivalent magnetic current sheets (because the

field inside the closed equivalent surface is zero). Thus, the lossy conductor is continued under the magnetic current sheet, which can be easily handled analytically.

Using the multilayer Green's functions of [21], with the details for this particular type of geometry (with magnetic current) in [16], we can find the expressions for $\bar{H}_1$ and $\bar{H}_2$. The finite conductivity of the conducting plane, and its finite thickness, can be treated via the general multilayer Green's function by regarding the conducting plane as a thin layer with a complex dielectric constant, $\epsilon = \epsilon_0 - j\sigma/\omega$. It should be noted that $\bar{H}_1$ and $\bar{H}_2$ should be computed, in general, as arising from the two magnetic currents on the two sides of the lossy conductor to account for field penetration through the conductor. Simplifications can, however, be made if the metal layer is thicker than several skin depths when the fields on the two sides of the conductor are isolated from each other and thus depend only on the magnetic current source on each side. In this case the required Green's function is due to a magnetic current on a lossy ground plane of semi-infinite extent in the normal direction and of infinite extent in the lateral direction.

In order for $\bar{M}$ or, equivalently, $\bar{E}$ to be the eigenfields of the transmission line, continuity of $\bar{H}_1$ and $\bar{H}_2$ should be enforced across the slot:

$$\bar{H}_1 - \bar{H}_2 = 0. \tag{8}$$

This magnetic field continuity condition can be implemented by Galerkin's testing as (eq. (1)):

$$\sum_{i=1}^{N} I_i \int_{j\text{th mode}} (\bar{H}_{1i} - \bar{H}_{2i}) \cdot (\bar{E}_j^* \times \hat{z})\, dy = \sum_{i=1}^{N} I_i Z_{ij} = 0 \tag{9}$$

where $\bar{E}_j$ is the jth slot electric field basis function, and the subscript i corresponds to tangential fields arising from the ith basis function with amplitude I_i. Spectral-domain implementation of (9) is straightforward using the Green's functions discussed. For the most general case with finite thickness and finite conductivity,

$$Z_{ij} = \int_{j\text{th mode}} \left[\left(\bar{\bar{\tilde{G}}}_{H_1 M} - \bar{\bar{\tilde{G}}}'_{H_1 M} \right) \cdot \bar{\tilde{M}}_i + \left(\bar{\bar{\tilde{G}}}_{H_2 M} - \bar{\bar{\tilde{G}}}'_{H_2 M} \right) \cdot \bar{\tilde{M}}_i \right] \cdot \left(\bar{\tilde{E}}_j^* \times \hat{z} \right) dk_y \tag{10}$$

where the primed Green's functions are for the respective magnetic fields caused by the magnetic source below the conductor, and the unprimed Green's functions are from the magnetic source above the conductor. It should be clear that when the metal is thick, because there is no coupling of the field from one side of the metal to the other,

$$\bar{\bar{\tilde{G}}}_{H_2 M} = \bar{\bar{\tilde{G}}}'_{H_1 M} = 0. \tag{11}$$

C. Integration Contour for Spectral Integrals

1) The Pole Consideration: Usually, the spectral integrals for Z_{ij} are evaluated along the real axis of the complex spectral plane. In this case Fourier transforms of various field components exist along the real spectral axis, and no possible branch cuts are crossed by the contour of integration. But when any source-free characteristic mode of the layered structure is excited, the fields of the leaky infinite-length transmission line exponentially increase in transverse directions. As shown in [15], this leakage effect occurs for cases where the guide propagation constant, β, is less than that of the characteristic mode, k_c. For example, in a conductor-backed slotline (see Fig. 3) the effective dielectric

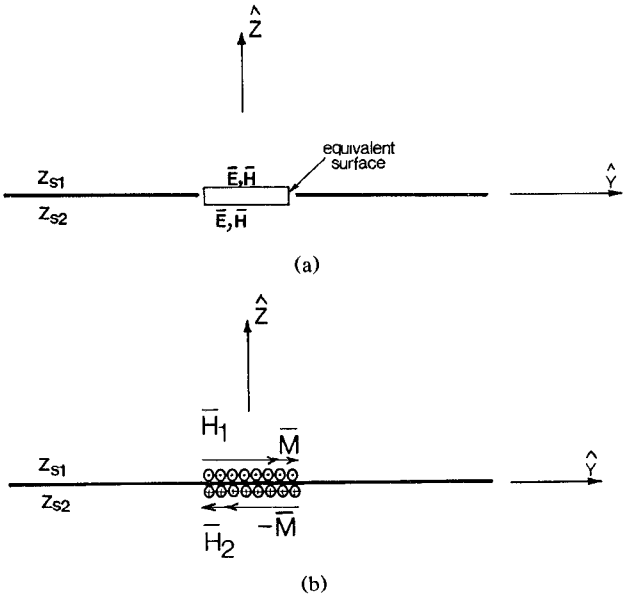

Fig. 2. Equivalent problem for a slotline on a lossy ground plane. (a) Original problem. (b) Equivalent problem.

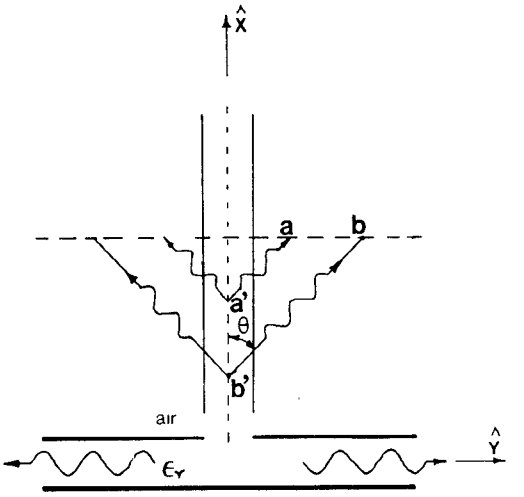

Fig. 3. Conductor-backed slotline that leaps power to parallel-plate mode.

constant, ϵ_{eff}, of the slotline is between ϵ_r and 1, where $k_c = k_0\sqrt{\epsilon_r} > (\beta = k_0\sqrt{\epsilon_{\text{eff}}}) > k_0$. The characteristic parallel-plate propagation constant, $k_t = k_0\sqrt{\epsilon_r}$, is unconditionally greater than β, which results in an unconditional leakage effect, independent of frequency or parallel-plate thickness. The attenuation constant due to leakage, α, is controlled by the parallel-plate thickness and the slot width, which results in a complex guide propagation constant, $k_c = \beta - i\alpha$.

Now, using the conductor-backed slotline as an example, the propagation of the excited characteristic wave in the y direction, given by $e^{-jk_{yp}y}$, should be such that

$$k_{yp} = \sqrt{k_c^2 - k_c^2} = \sqrt{k_c^2 - \beta^2 + \alpha^2 + 2j\beta\alpha}. \tag{12}$$

It can be easily checked that k_{yp} may lie in the first quadrant (or third quadrant, due to its double value) of the complex plane, which corresponds to a propagation and exponential growth in the outward direction. This exponen-

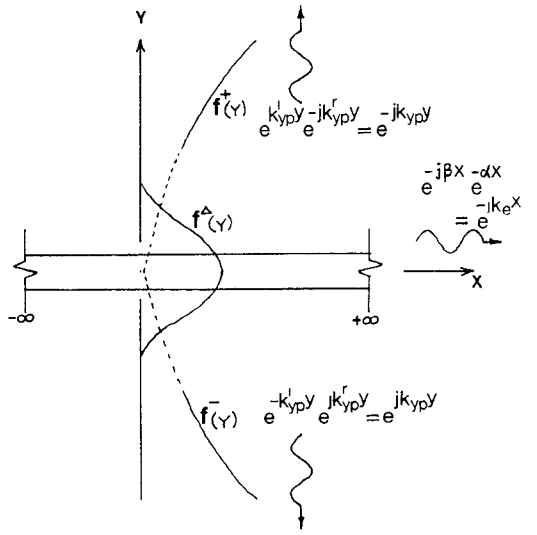

Fig. 4. Transverse variation (even type) of fields of an infinite leaky transmission line.

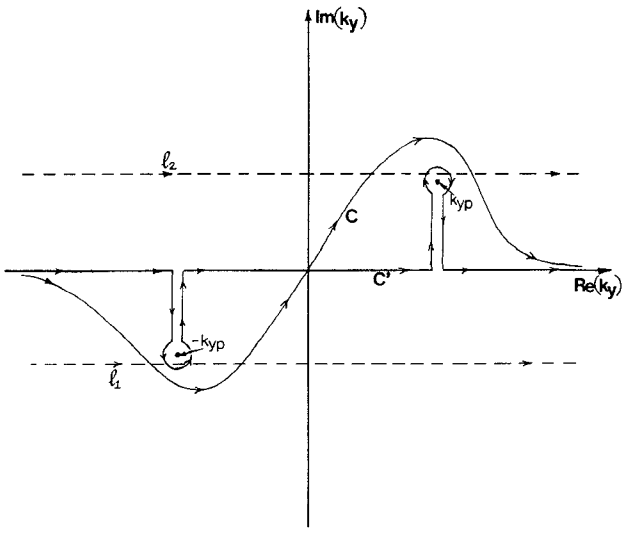

Fig. 5. Integration contours on complex k_y plane for a transmission line with leakage to characteristic surface wave.

tial growth in the transverse direction can be qualitatively explained as follows.

As shown in Fig. 3, the points a and b receive the characteristic waves originating respectively from the points a' and b' along the slot, where $\theta = \cos^{-1}(k_e/k_c)$ [15] (this is strictly not true for a complex lossy k_e, but provides a fairly good qualitative picture for small loss). When the slotline is lossy because of the leakage effect, the electric field on the slotline has an exponential decay along the propagation direction, resulting in a larger value at b' than at a'. Hence the field magnitude at b tends to be larger than that at a, which explains an increasing trend of the electric field in the transverse direction. In fact, it is true in general that, for a multilayered structure, a guided mode with propagation constant smaller than that of a characteristic mode of the structure always leaks power and results in exponentially growing fields in the transverse direction. Clearly, for such an exponentially growing field component, the Fourier transform in the y direction does not exist for real values of spectral arguments, k_y.

In order to handle this problem in the spectral domain, we decompose any field or potential of the transmission line, $f(y)$, into three parts (see Fig. 4):

$$f(y) = f^+(y) + f^-(y) + f^\Delta(y) \tag{13}$$

such that f^+ extracts the part of f that exponentially grows for $y \to \infty$, and f^- extracts the part of f that grows for $y \to -\infty$. For example, we can choose

$$f^+(y) = Ce^{k'_{yp}y} e^{-jk'_{yp}y} u(y) = e^{-jk_{yp}y} u(y) \tag{14}$$

$$f^-(y) = \pm Ce^{-k'_{yp}y} e^{+jk'_{yp}y}(1-u(y)) = e^{+jk_{yp}y}(1-u(y)) \tag{15}$$

with $\pm C$ for odd or even symmetry of the respective field, $k^r_{yp} > 0$, $k'_{yp} > 0$, and $u(y) = 1$ for $y > 0$ and zero for $y < 0$.

Now with this decomposition, $f^\Delta(y)$ does not grow in the transverse directions; thus its Fourier transform exists on the real spectral axis. The Fourier transforms of $f^+(y)$ and $f^+(y)$ in (14) and (15) can be expressed as

$$F^+(k_y) = \frac{C}{j(k_y + k_{yp})}, \qquad \mathrm{Im}(k_y) < -k'_{yp} \tag{16}$$

$$F^-(k_y) = \frac{\pm C}{-j(k_y - k_{yp})}, \qquad \mathrm{Im}(k_y) > -k'_{yp}. \tag{17}$$

It should be noted that the transforms, F^+ and F^-, in (16) and (17) contain poles at $-k_{yp}$ and k_{yp} respectively. In fact, instead of the f^+ and f^- expressions of (14) and (15), if any other f^+ and f^- expressions were chosen to extract the exponential growing behavior, the corresponding F^+ and F^- spectral expressions would contain poles of first order at $-k_{yp}$ and k_{yp} respectively. Thus, because the spectral-domain poles of the total field expression, $F(k_y)$, at these locations are also of first order [14], they are completely extracted into F^+ and F^-. The remaining spectral content, F^Δ, is therefore analytic everywhere in the complex k_y plane. (This assumes, however, that only one characteristic mode exists, but the argument can be extended for additional characteristic modes.)

Owing to the nature of the individual components, F^+, F^- and F^Δ, the respective inverse integral contours are restricted. Because F^Δ is analytic everywhere in the complex k_y plane, the spectral integration contour can be along any path from $-\infty + j0$ to $+\infty + j0$. On the other hand, the required contours for F^+ and F^-, as required by the conditions of (16) and (17), need to be along any horizontal line below and above the lines, l_1 and l_2, respectively (see Fig. 5). By suitable analytic deformation, the contours for F^+ and F^- can, however, be chosen to be any curved line traversing below and above the poles at $-k_{yp}$ and k_{yp} respectively. The contour, C, that satisfies the existence and validity of transforms of all three components of F should be such that it contains $-k_{yp}$ and k_{yp} respectively above and below it (see Fig. 5). By further deforming C in Fig. 5, we obtain a simple contour C' that covers the entire real axis and encloses $-k_{yp}$ and k_{yp} in the residue sense.

In the moment method formulation, when the Z_{ij}'s are computed as reactions of different field quantities on the test functions, the spectral integrals contain the Green's func-

tions for the field components (the field transform of a line source) and transforms of the finite domain basis functions. Since the transforms of finite domain functions are always analytic over the entire complex spectral plane, the integration contours of these spectral integrals are determined by the analyticity and pole locations of the Green's function alone. The spectral integrals need to be evaluated along C' (see Fig. 5) and can be simplified to

$$\int_{-\infty}^{\infty}(\cdot)\,dk_y + 2\pi j\left[\mathrm{Res}(\cdot)_{-k_{yp}} - \mathrm{Res}(\cdot)_{k_{yp}}\right]. \quad (18)$$

It should be noted, that a leaky infinite-length transmission line with growing fields in the transverse direction does not fundamentally violate the radiation condition. The radiation condition in electromagnetic theory is based on the assumption of finiteness of radiated power in the far field owing to a source of finite power. This is not the case for an ideal infinite-length leaky line, because the source power itself (with $e^{-\alpha x}$ variation along the line) is infinite at $x = -\infty$.

However, it may seem unreasonable that in practice a leaky transmission line has growing fields in its transverse direction. A practical transmission line, in fact, does not have growing electric fields in its transverse direction, owing to its finite length and finite substrate size, in contrast to an ideal infinite-length line on a substrate of infinite size assumed in our analysis. Nevertheless, such a practical finite-length leaky transmission line would definitely have larger spreading of its fields, as opposed to the tightly bound guided fields of other nonleaky structures. The widely spreading unbound fields get scattered off the edges of the substrates of finite size. And thus, because of the interference of the scattered fields, the characteristics of the leaky practical transmission lines on substrates of finite size would be more likely to deviate from the characteristics obtained from the ideal infinite-structure analysis. This is in contrast to cases of nonleaky geometries that do not practically see the far-off edges of finite-size substrates. The propagation characteristics of an infinite-length ideal leaky transmission line still provide useful information for these finite-length transmission lines.

2) Branch Cut and Branch Plane Consideration: It should be noted that in the preceding discussion of complex spectral plane integration it was assumed that any analytic deformation of the integration contour should lie on the same branch plane. Multiple branch planes occur in the complex plane of spectral-domain Green's functions for a layered geometry if the top or the bottom layer of the multilayer structure is infinite in the normal direction [16], into which power can radiate. Mathematically, these spectral-domain branch cuts are due to multivalued square root expressions for outward propagation in the infinite mediums. The value of the outward propagation constant is chosen [23] such that it corresponds to a decaying wave, which is consistent with the radiation condition. It may be mentioned that similar multivalued square root expressions occur in the spectral Green's functions for propagation in other finite-thickness layers of a multilayered geometry, but these can be shown not to correspond to any valid branch cut, and are removable in the final Green's function expression [16].

These branch cuts are, however, of particular importance when one considers the case of an infinite planar transmission line leaking power to radiation. Like the condition for leakage to a surface mode for a planar transmission line on a general multilayered medium, radiation leakage occurs when the real propagation constant of the transmission line mode

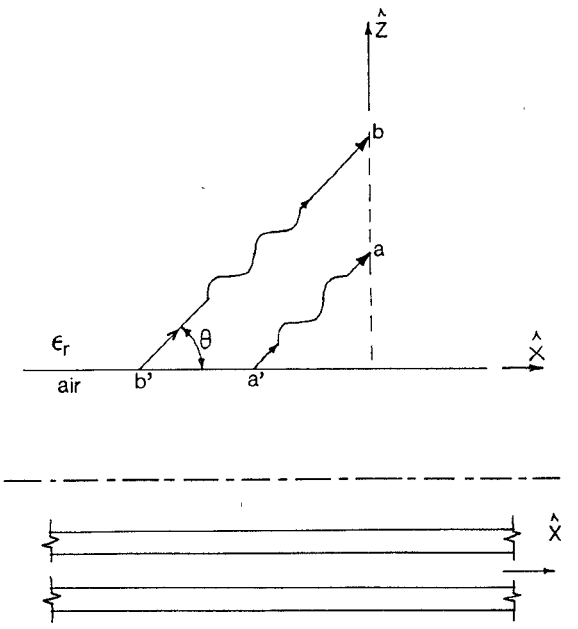

Fig. 6. Radiation leakage in a coplanar stripline at the interface between two semi-infinite mediums.

is less than that of an infinitely extending layer on top or bottom. For example, the dominant mode of a coplanar stripline on the interface of two semi-infinite layers, air and a semi-infinite dielectric layer (see Fig. 6), has a propagation constant between those of the two mediums, which is less than the propagation constant of the dielectric medium. So, as discussed, the coplanar stripline is lossy owing to leakage to radiation into the dielectric medium. In contrast to the leakage caused by characteristic mode excitation, where the power leaks in only one direction, corresponding to only one characteristic mode propagation constant, the radiation leakage occurs over a spectrum of wavenumbers from zero to $k_0\sqrt{\epsilon_r}$, which corresponds to conical radiations from the transmission line given by the cone angle, $\theta = \cos^{-1}(k_e/k_0\sqrt{\epsilon_r})$ (see Fig. 6) [17]. (This again is not rigorously true for complex lossy k_e but provides a fairly good qualitative picture for low-loss cases.)

Also, with similar arguments to explain the exponential growth of the electric field in transverse directions for the characteristic wave leakage case, one can explain in this case a nondecaying field in the normal direction (see Fig. 6). This seems to violate the radiation condition of electromagnetics discussed earlier; hence interpretation of a proper choice of branch cut and branch plane for outward propagation is important. However, like the characteristic wave leakage case, the fundamental principle of finiteness of radiated power at far field owing to a source of finite power is not violated because the input power at $x \to -\infty$ (for $e^{-\alpha x}$ variation) is infinite. All other arguments for the practicality and significance of the growing electric field with distance caused by an $e^{-\alpha x}$ variation along a transmission line with the characteristic wave leakage also apply here for the radiation leakage.

This condition of growing electric fields in normal directions is incorporated into the solution by a proper choice of branch cuts and branch planes. For such a structure ($\mathrm{Re}(k_e) < k_0\sqrt{\epsilon_r}$) the branch points in the complex k_y plane are

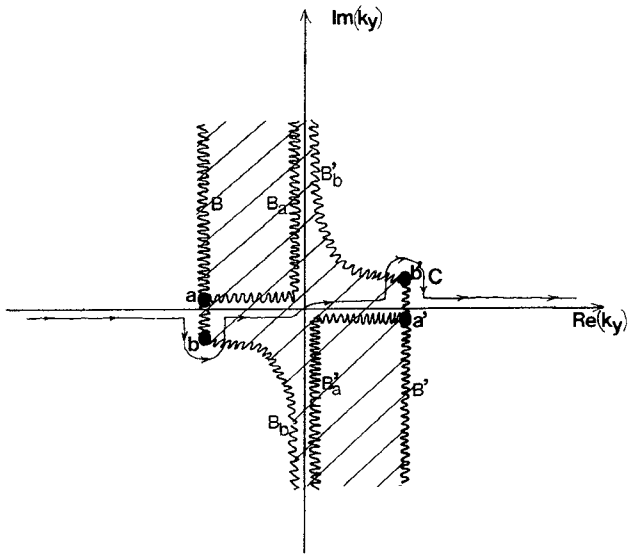

Fig. 7. Integration contour and branch cuts in the complex k_y plane for a lossy transmission line with radiation leakage.

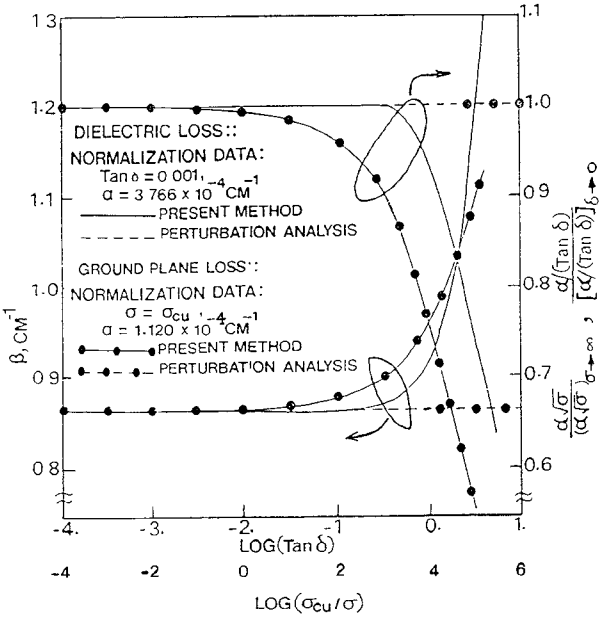

Fig. 8. Comparison of ground plane and dielectric losses of a microstrip line computed by present method and by the perturbation method. Substrate: $\epsilon_r = 2.2$, 0.16 cm, line width = 0.5 cm, freq = 3.0 GHz, no loss effective propagation constant = 0.866 cm^{-1}. Ground plane conductivity = σ, substrate loss tangent = $\tan\delta$.

shown in Fig. 7 as a and a', given by $k_y = \sqrt{k_0^2\epsilon_r - k_e^2}$, for k_e without loss (but ϵ_r with slight loss, which is realistic). In this lossless case the choice of branch cuts is arbitrary as long as the real k_y axis of integration satisfies the radiation condition (for lossless k_e) and does not cross the branch cut. The vertical lines in Fig. 7 originating at a and a' and continuing up and down, respectively, form a pair of such branch cuts. For analysis of finite structures (antennas), alternative branch cuts, B_a and B_a', are chosen [23] such that the entire branch plane satisfies the radiation condition. But these branch cuts are not suitable for extending the analysis for lossy k_e cases, where this radiation condition is no longer valid. When k_e becomes leaky the branch point can be seen to move from the fourth to the first quadrant, and from the second to the third quadrant with the branch cuts, B and B', now cutting across the real k_y axis. In order to maintain analytic continuity of the physical situation of gradual transition from the lossless to the lossy case, the contour of integration needs to be deformed around the branch cut on the same branch plane (contour C of Fig. 7). An exact physical interpretation of this deformation seems to be difficult at this point but is consistent with the fact that the contour of integration partly covers a region that does not satisfy the radiation condition (the shaded portion of the presently chosen branch plane corresponding to the branch point pair, (b, b'), does not satisfy the radiation condition), which accounts for the nondecaying fields in the normal direction. It should also be noted that if the branch cuts B_a and B_a' had been chosen, which eventually move to B_b and B_b' respectively for lossy k_e, the real k_y axis of integration (which now does not cross the branch cuts) would jump from one side of the branch cuts to the other, representing a discontinuous nonphysical condition that is invalid and nonanalytic.

D. Root Searching in the Complex Plane

The root searching for (2) in the complex k_e plane is computationally complex and time consuming. Also, the spectral integral for computation of Z_{ij} has to be evaluated for complex values of the spectral parameter k_x, which is often difficult. However, for most practical cases of small loss, the problem can be simplified to root searching along the real k_e axis only. If there is no loss, $\mathrm{Det}[k_e]$ of (2) is equal to zero for a real value of $k_e = \beta$. With the addition of small loss, $\mathrm{Det}[\beta] = u$, where u is a small complex number in general. Then we compute the determinant in the neighborhood of β, i.e., $k_e = \beta + \Delta\beta$, and let $\mathrm{Det}(\beta + \Delta\beta) = v$, where v is also complex in general. With these two values of the determinant for two closely spaced points on the real axis, we can obtain the complex solution for $\mathrm{Det}[k_e = \beta - j\alpha]$ by analytic extrapolation, where $\alpha = (-ju\Delta\beta)/(v - u)$. This method is referred to as the spectral-domain perturbation method, where a perturbation of the spectral integrals is implemented, in contrast to the commonly used space-domain perturbation method, where the spatial field distributions are perturbed by the loss caused by the finite conductivity of a real conductor or nonzero loss tangents of real dielectrics. Both perturbation methods are valid only for small losses. But the spectral perturbation method obtains the loss together with the real propagation constant without additional computation. It is computationally simple and straightforward and, as discussed, is particularly important for multilayered geometries to avoid separately computing the perturbation loss contribution from all the loss elements, which is analytically involved as well as computationally complex and sometimes impractical.

III. Results and Discussions

A. Dielectric and Ground Plane Loss in a Microstrip

Fig. 8 compares the propagation and attenuation constants of a microstrip line with a lossy ground plane and lossy dielectric substrates as obtained from the present analysis and a perturbation analysis [11]. The results were obtained by incorporating ground plane and dielectric losses into the Green's functions and solving for the complex propagation constant. Strip loss was not included. As the results show,

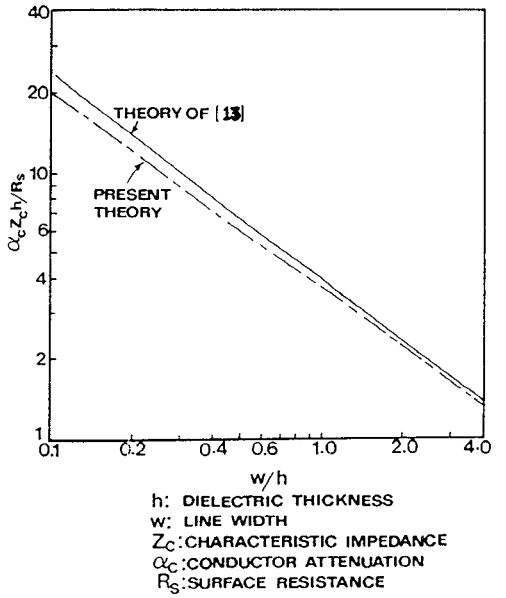

Fig. 9. Comparison of total conductor loss of a microstrip line including the center strip obtained using the present method and that of [13].

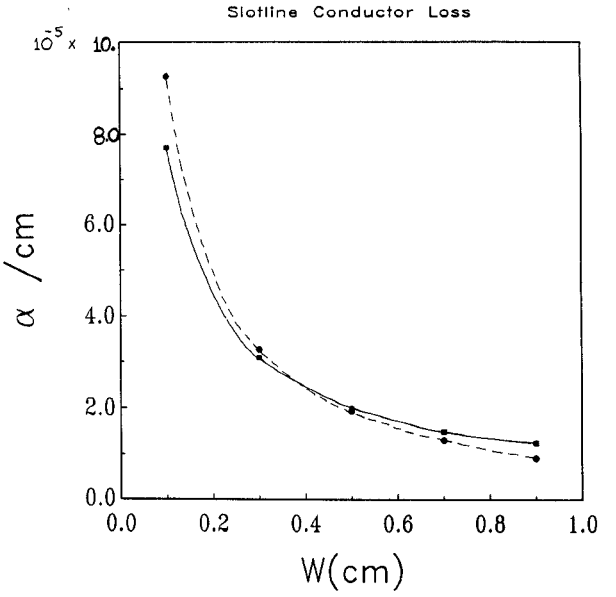

Fig. 10. Comparison of total conductor loss of a slotline using the present method (——) and the space-domain perturbation method (----), as a function of width, w; frequency = 3.0 GHz, dielectric constant = 2.55.

the perturbation analysis provides quite accurate results for fairly large values of loss tangents or ground plane resistivity. The loss tangent can be as high as approximately 0.1 for the perturbation analysis to be valid. It is, however, more critical for ground plane conductivity. For this particular parameter set the perturbation analysis starts to show deviation from the full-wave results for conductivity values as low as one hundredth of the conductivity of copper. This limit is still worse for larger frequencies (varies as square root of frequency) and also if the strip loss is included.

B. Strip Loss of Microstrip Line and Ground Plane Discontinuity Loss of Slotline

Using the proper boundary conditions discussed in the last section, losses in a microstrip line caused by the strip conductor, and in a slotline caused by the ground plane's slot edge discontinuity, are calculated. In the microstrip line case, conductor loss arising from the infinite ground plane is also added via the Green's functions with an impedance boundary. The results are presented in Figs. 9 and 10, respectively. Results for the microstrip line are compared with those of the widely used static analysis of [13]. The agreement is fairly close except for small strip widths. For the slotline, the results are compared with those of a separately formulated perturbation analysis (Fig. 10). The agreement is equally good, but it experiences a much weaker convergence with respect to the number of expansion functions used compared with that for a microstrip line strip loss analysis.

C. Parallel-Plate Mode Leakage in a Conductor-Backed Slotline

The results of the propagation and attenuation constants of a conductor-backed slotline are compared in Fig. 11 with the theory and experiment of [15]. This incorporates proper deformation of the spectral integration contour to include the pole caused by the parallel-plate mode. The agreement between the different results of Fig. 11 is generally good, and

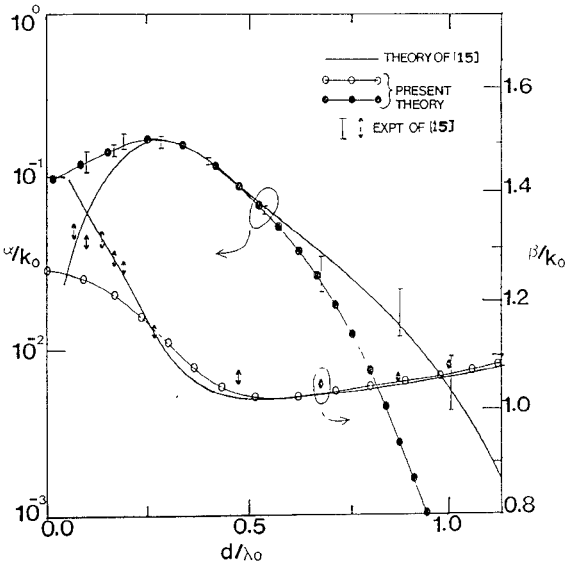

Fig. 11. Propagation constant (β) and attenuation constant (α) of a conductor-backed slotline compared with the results of [15]. Parallel-plate substrate: $\epsilon_r = 2.55$, thickness = b, $b/\lambda_0 = 0.267$, slot width = d, freq = 10 GHz.

there is qualitative agreement with the experimental results except for low and high values of d/λ_0. For large values of d/λ_0, the number of basis functions for expansion of the transverse variation of the slot field required for the present analysis is extremely large, which could explain the deviation of the results from the theory of [15] owing to insufficient convergence. The deviation of the results for smaller d/λ_0, however, is not clear.

As shown in Fig. 11 the leakage loss in a conductor-backed slotline can be reduced by increasing the slot width or by increasing the parallel-plate thickness. It can also be avoided by loading the slotline with a substrate of sufficiently high dielectric constant on the top. This would result in increasing

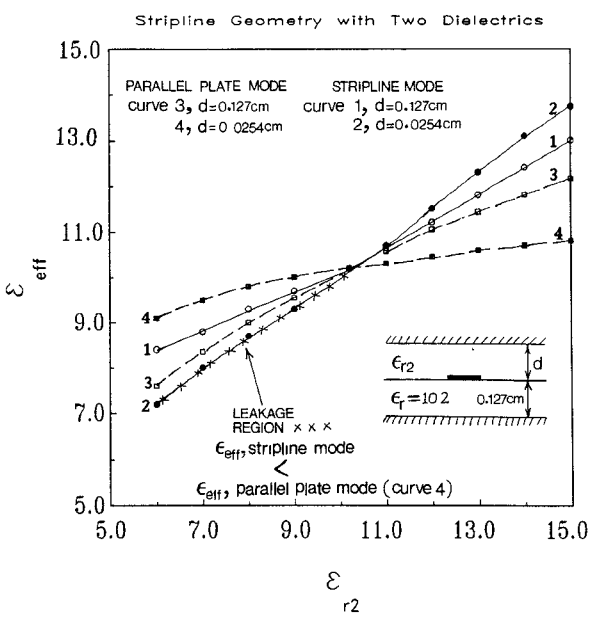

Fig 12. Effective dielectric constants, ϵ_{eff}, of the characteristic two-layer parallel-plate mode compared with that of the two-layer stripline mode, as a function of the dielectric constant of one layer, ϵ_{r2}, to demonstrate the new leakage effect. Frequency = 3.0 GHz, strip width = 0.12 cm.

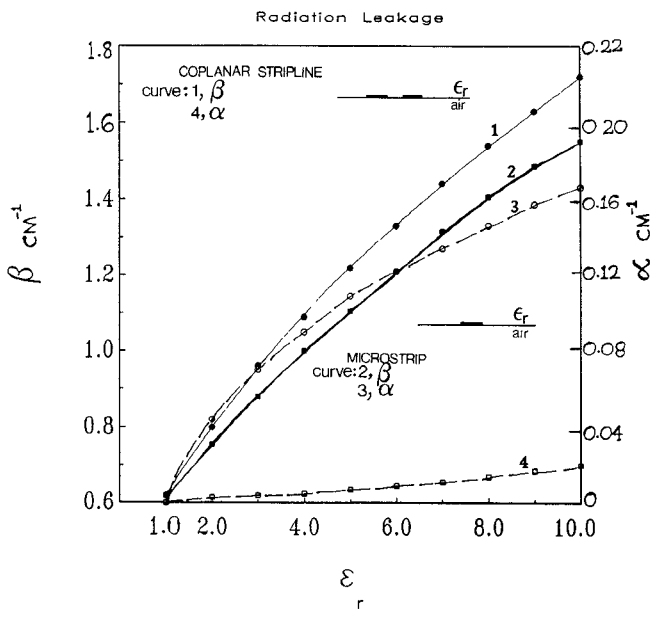

Fig. 13. Propagation (β) and attenuation (α) constants of a coplanar stripline and a microstrip line at the interface between a semi-infinite dielectric medium and air. Coplanar stripline: width = 0.5 cm, center-to-center line separation = 0.6 cm; microstrip line: width = 0.5 cm; frequency = 3.0 GHz.

the dominant mode propagation constant above that of the parallel-plate mode and, as discussed before, would eliminate the excitation of the characteristic mode.

D. A Potential Leakage Effect in a Stripline with Two Dielectrics

A leakage effect similar to that in a conductor-backed slotline described above occurs for the dominant mode of a stripline geometry with two different dielectrics. As shown in Fig. 12, for the case where the two substrates are of the same thickness, the stripline mode has a propagation constant, $k_0\sqrt{\epsilon_{eff}}$ (curve *1*), always greater than or equal to the corresponding characteristic parallel-plate mode (curve *3*). On the other hand, when the two substrates are of different thicknesses and the thicker substrate has a larger dielectric constant (curve *2*, crossed region), the stripline propagation constant is less than that of the characteristic parallel-plate mode (curve *4*). For this case, the electric field of the stripline is concentrated on the thin substrate (with smaller dielectric constant), which makes its effective dielectric constant closer to that of the thin substrate. The effective dielectric constant of the parallel-plate mode, however, is dominated by the thicker substrate, and so it tends to be larger than that of the stripline mode. This condition, as described before, excites the parallel-plate mode, resulting in a leaky stripline.

E. Radiation Leakage in a Microstrip Line or a Coplanar Stripline on a Semi-Infinite Dielectric

The propagation and attenuation constants of a microstrip line and a coplanar stripline on a semi-infinite dielectric medium are presented in Fig. 13. As discussed previously, the power leaks to radiation into the dielectric medium, and this effect is incorporated into the solution by proper selection of the branch cut and deformation of the spectral integration contour. Clearly, the leakage increases for larger dielectric constants, with no leakage when the dielectric constant is unity, as expected. The leakage in a coplanar stripline is comparatively less than that in a microstrip because of cancellation of radiation caused by the oppositely directed currents on the two odd-mode strips of the coplanar stripline structure.

IV. Conclusions

Several geometries have been analyzed for material and leakage losses using the general multilayer loss analysis described in this paper. Results are compared with other results from the literature, where available. This paper provides, for the first time, a full-wave spectral analysis of the parallel-plate leakage loss in a conductor-backed slotline and of the radiation losses in striplines at the interface of two semi-infinite mediums. Furthermore, it identifies a potential leakage loss in a two-layer stripline. The general analysis will find potential use for the prediction or full-wave quantification of leakage and material losses in other layered geometries for multilayered integrated circuit applications.

Acknowledgment

The authors acknowledge many helpful discussions with Prof. R. W. Jackson of the University of Massachusetts, Amherst.

References

[1] R. J. Mailloux, "Phased array architectures for millimeter wave active arrays," *IEEE Antennas and Propagation Society Newsletter*, vol. AP-28, no. 1, pp. 5–7, Feb. 1986.

[2] N. K. Das and D. M. Pozar, "Printed antennas in multiple layers: General considerations and infinite array analysis using

a unified method," in *Proc. IEE Int. Conf. Antennas and Propagat.*, ICAP, (University of Warwick, UK), Apr. 1989, pp. 364–368.
[3] J. A. Kinzel, "GaAs technology for millimeter wave phased arrays," *IEEE Antennas and Propagation Society Newsletter*, vol. AP-29, pp. 12–14, Feb. 1987.
[4] D. S. Phatak, N. K. Das, and A. Defonzo, "Dispersion characteristics of optically excited coplanar striplines: Comprehensive full-wave analysis," *IEEE Trans. Microwave Theory Tech.*, vol. 38, pp. 1719–1730, Nov. 1990.
[5] D. S. Phatak and A. Defonzo, "Dispersion characteristics of optically excited coplanar striplines: Picosecond pulse propagation," *IEEE Trans. Microwave Theory Tech.*, vol. 38, pp. 654–661, May 1990.
[6] E. J. Denlinger, "A frequency dependent solution for microstrip transmission lines," *IEEE Trans. Microwave Theory Tech.*, vol. MTT-19, pp. 30–39, Jan. 1971.
[7] T. Itoh and R. Mittra, "Spectral domain approach for calculating the dispersion characteristics of microstrip lines," *IEEE Trans. Microwave Theory Tech.*, vol. MTT-21, pp. 496–499, July 1973.
[8] J. B. Davies and D. Mirshekar-Syahkal, "Spectral domain solution of arbitrary transmission line with multilayer substrate," *IEEE Trans. Microwave Theory Tech.*, vol. MTT-25, pp. 143–146, Feb. 1977.
[9] Y. Fukuoka, Y. Shih, and T. Itoh, "Analysis of slow-wave coplanar waveguide for monolithic integrated circuits," *IEEE Trans. Microwave Theory Tech.*, vol. MTT-31, pp. 567–573, July 1983.
[10] R. W. Jackson, "Considerations in the use of coplanar waveguide for millimeter-wave integrated circuits," *IEEE Trans. Microwave Theory Tech.*, vol. MTT-34, pp. 1450–1456, Dec. 1986.
[11] D. Mirshekar-Syahkal and J. B. Davies, "Accurate solution of microstrip and coplanar structures for dispersion and for dielectric and conductor losses," *IEEE Trans. Microwave Theory Tech.*, vol. MTT-27, pp. 694–699, July 1979.
[12] E. J. Denlinger, "Losses of microstrip lines," *IEEE Trans. Microwave Theory Tech.*, vol. MTT-28, pp. 513–522, June 1980.
[13] R. A. Pucel, D. J. Masse, and C. P. Hartwig, "Losses in microstrip," *IEEE Trans. Microwave Theory Tech.*, vol. MTT-16, pp. 342–350, June 1968.
[14] T. Mu, H. Ogawa and T. Itoh, "Characteristics of multiconductor, asymmetric, slow-wave microstrip transmission lines," *IEEE Trans. Microwave Theory Tech.*, vol. MTT-34, pp. 1471–1477, Dec. 1986.
[15] H. Sigesawa, M. Tsuji, and A. A. Oliner, "Conductor backed slotline and coplanar waveguide: Dangers and full-wave analysis," in *IEEE MTT-S Int. Microwave Symp. Dig.*, 1988, pp. 199–202.
[16] N. K. Das, "A study of multilayered printed antenna structures," Ph.D. dissertation, Dept. Electrical and Computer Engineering, Univ. Massachusetts, Amherst, Sept. 1989.
[17] D. B. Rutledge, D. P. Neikirk, and D. P. Kasilingam, "Planar integrated circuit antennas," ch. 1, vol. 10, *Millimeter Components and Techniques*, Part II of *Infrared and Millimeter Waves*, K. J. Button, Ed. New York: Academic Press, 1983.
[18] A. A. Oliner and K. S. Lee, "The nature of the leakage from higher modes on microstrip line," in *IEEE MTT-S Int. Microwave Symp. Dig.*, 1986, pp. 57–66.
[19] K. A. Michalski and D. Zheng, "Rigorous analysis of open microstrip lines of arbitrary cross section in bound and leaky regimes," *IEEE Trans. Microwave Theory Tech.*, vol. 37, pp. 2005–2010, Dec. 1989.
[20] J. S. Bagby, C. H. Lee, D. P. Nyquist, and Y. Yuan, "Propagation regimes on integrated microstrip transmission lines," presented at National Radio Science Meeting, Boulder, CO, Jan. 1990.
[21] N. K. Das and D. M. Pozar, "Generalized spectral-domain Green's function for multilayer dielectric substrates with applications to multilayer transmission lines," *IEEE Trans. Microwave Theory Tech.*, vol. MTT-35, pp. 326–335, Mar. 1987.
[22] T. E. Deventer, P. B. Katehi, and A. C. Cangellaris, "An integral equation method for the evaluation of conductor and dielectric losses in high frequency interconnects," *IEEE Trans. Microwave Theory Tech.*, vol. 37, pp. 1964–1973, Dec. 1989.
[23] D. M. Pozar, "Input impedance and mutual coupling of rectangular microstrip antennas," *IEEE Trans. Antennas Propagat.*, vol. AP-30, pp. 1191–1196, Nov. 1982.

✠

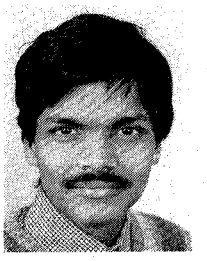

Nirod K. Das was born in Puri, Orissa state, India, on February, 27, 1963. He received the B. Tech(Hons.) degree in electronics and electrical communication engineering from the Indian Institute of Technology (IIT), Kharagpur, India, in 1985 and the M.S. and Ph.D. degrees in electrical engineering from the University of Massachusetts, Amherst, in 1987 and 1989 respectively.

He worked in the Department of Electrical and Computer Engineering at the University of Massachusetts, Amherst, from 1985 to 1989 as a Graduate Research Assistant, and then as a Post-Doctoral Research Associate after completion of his Ph.D. degree. Presently he is an Assistant Professor at the Polytechnic University, Farmingdale, New York. His research interests are in the general areas of microwave and millimeter-wave integrated circuits and antennas, in particular, the analytical and experimental study of multiple-layer integrated circuit structures for phased array applications.

✠

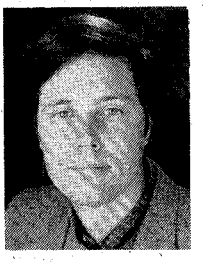

David M. Pozar (S'74–M'80–SM'88–F'90) was born in Pittsburgh, PA, in 1952. He received the B.S. degree in 1975 and the M.S. degree in 1976, both in electrical engineering, from the University of Akron, Akron, OH. He received the Ph.D. degree from Ohio State University in 1980.

During the course of his undergraduate studies, he spent one year as an Engineering Assistant at the National Security Agency, Fort Meade, MD. He was a Graduate Research Assistant at the ElectroScience Lab of Ohio State University while pursuing the Ph.D. degree, and became a Research Assistant upon completion of the degree. He joined the faculty of the University of Massachusetts in 1980, and in 1989 became Professor of Electrical and Computer Engineering. In 1988 he spent a six-month sabbatical leave at Ecole Polytechnique Federale de Lausanne, Lausanne, Switzerland, participating in several short courses and workshops on printed antennas.

Dr. Pozar is an associate member of the International Union of Radio Science (URSI), Commission B. He has served as an Associate Editor of the IEEE TRANSACTIONS ON ANTENNAS AND PROPAGATION (1983–1986) and as an Associate Editor of the *IEEE Antennas and Propagation Society Newsletter* (1982–1984). In 1981 he received the "Outstanding Professor for 1981" award from Eta Kappa Nu, the student honor society. In 1984 he received an NSF Presidential Young Investigator Award, as well as the "Keys to the Future Award" from the IEEE Antennas and Propagation Society. In 1985 he received the Engineering Alumni Association "Outstanding Junior Faculty Award." In 1986 he received the R. W. P. King Best Paper Award from the IEEE Antennas and Propagation Society. In 1987 he received the URSI Issac Koga Gold Medal for his work on printed antennas and phased arrays. He again received the R. W. P. King Best Paper Award in 1988. In 1989 he received the United Technologies Corporation "Outstanding Teaching Award." He presently serves as an Associate Editor for the IEEE TRANSACTIONS ON ANTENNAS AND PROPAGATION. Besides publishing papers on printed antennas and phased arrays, Dr. Pozar is the author of *Antenna Design Using Personal Computers* (Artech House, 1985), and *Microwave Engineering* (Addison-Wesley, 1990).